

Article

Experimental Study on the Hygrothermal Behavior of a Coated Sprayed Hemp Concrete Wall

Thibaut Colinart *, Patrick Glouannec, Thomas Pierre, Philippe Chauvelon and Anthony Magueresse

Laboratoire d'Ingénierie des MATériaux de Bretagne (LIMATB), Université de Bretagne-Sud, Université Européenne de Bretagne, Rue de Saint Maudé, BP 92116, 56321 Lorient Cedex, France; E-Mails: patrick.glouannec@univ-ubs.fr (P.G.); thomas.pierre@univ-ubs.fr (T.P.); philippe.chauvelon@univ-ubs.fr (P.C.); anthony.magueresse@univ-ubs.fr (A.M.)

* Author to whom correspondence should be addressed; E-Mail: thibaut.colinart@univ-ubs.fr; Tel.: +33-297-874-517; Fax: +33-297-874-619.

Received: 29 November 2012; in revised form: 4 January 2013 / Accepted: 11 January 2013 / Published: 18 January 2013

Abstract: Hemp concrete is a sustainable lightweight concrete that became popular in the field of building construction because of its thermal and environmental properties. However, available experimental data on its hygrothermal behavior are rather scarce in the literature. This paper describes the design of a large-scale experiment developed to investigate the hygrothermal behavior of hemp concrete cast around a timber frame through a spraying process; and then coated with lime-based plaster. The equipment is composed of two climatic chambers surrounding the tested wall. The experiment consists of maintaining the indoor climate at constant values and applying incremental steps of temperature; relative humidity or vapor pressure in the outdoor chamber. Temperature and relative humidity of the room air and on various depths inside the wall are continuously registered during the experiments and evaporation phenomena are observed. The influence of the plaster on the hygrothermal behavior of hemp concrete is investigated. Moreover, a comparison of experimental temperatures with numerical results obtained from a purely conductive thermal model is proposed. Comparing the model with the measured data gave satisfactory agreement.

Keywords: bio-based material; lime plaster; multilayer wall; large-scale experiment; temperature and relative humidity measurement; coupled heat and moisture transfer; evaporation; moisture accumulation; 1D thermal simulation

1. Introduction

Nowadays, a large number of works deal with hygroscopic building materials in order to understand their hygrothermal performance in the building envelope and their interaction with enclosed space. In this view, numerical studies have shown positive effect on building energy demand [1], on HVAC (heating, ventilation, and air conditioning) system energy consumption in dwelling buildings [2,3] or on indoor air quality in buildings by reducing the amplitude of daily moisture variations [4,5]. Most of these studies are based on the description of HAM (heat, air and moisture) transport within the material. One of the difficulties in HAM simulation is to obtain an accurate knowledge of transport properties [6,7]. For example, moisture (in liquid or in vapor form) contained within the hygroscopic material may influence its thermal properties. For that purpose, Hagentoft's [8] simple calculation of heat flow with and without moisture in a structure demonstrates that arbitrary choice of values for the thermal properties may result in an incorrect prediction of the building enclosure performance. This example confirms that validating the HAM models against experimental data is essential.

In this view, many experimental works are performed at different scales using several methods [9–15]. At the material scale, homogeneous samples have been well characterized for validation of coupled BES (Building Energy Simulation)-HAM models, as well as of CFD (Computational Fluid Dynamics) HAM models [9] or for investigation of specific phenomenon like temperature-driven inward vapor transport [10]. The methodology is well known and relatively cheap, but Van Belleghem *et al.* [9] point out that attention must be paid to control accurately the boundary conditions and to reduce influences from surroundings to a minimum. Furthermore, such experiment does not correspond faithfully to reality. At the building scale, experiments are longer, more expensive and require inserting sensors during building construction [11]. A good compromise lies therefore in studying large size (and sometimes heterogeneous) walls [12–15]. In this case, the boundary conditions may be well controlled either on both sides with a climatic or only on one side, the other side being subjected to the outdoor (or laboratory) conditions. This specific experiment allows investigation of the hygrothermal behavior as a function of combined and controlled heat, air and moisture fluctuations and thus creating a large database and benchmark for validating HAM models in order to accurately predict energetic behavior and overall comfort.

All these numerical and experimental methods are largely applied to classical hygroscopic building materials like gypsum, wood panels or insulation, but less to new sustainable materials, like hemp concrete, that may offer large possibilities in the sustainable building construction yet [16–18]. Indeed, this bio-based material formed from hemp shives and a lime-binder has a positive life cycle assessment [19], a low bulk density ($300 < \rho_b < 600 \text{ kg}\cdot\text{m}^{-3}$) [20], a high porosity ($n_f > 0.65$) [21–23] and a good effective thermal conductivity ($0.07 < \lambda_{\text{eff}} < 0.2 \text{ W}\cdot\text{m}^{-1}\cdot\text{K}^{-1}$) [22–25]. Furthermore, its hygric properties, like sorption/desorption curves, vapor permeability or moisture buffering capacity, are well characterized [23,26]. Nevertheless, even if hemp concrete properties are well known, there are few works dealing with the hygrothermal performance of hemp concrete. At the material scale, Colinart *et al.* [20] experimentally investigated the drying of hemp concrete and observed that manufacturing process influences the initial water content, and thus the drying time, and the final density whereas the hygrothermal behavior during the drying stage depends on the material formulation. At the building scale, Walker's research group [27] reported recent works on the

construction and the hygrothermal performance of experimental hemp–lime building and proposed a comparison of the results of steady-state co-heating tests with laboratory tests. Their results indicate that the temperature and humidity variations inside the house are significantly dampened compared with the external environment. For their part, Maalouf *et al.* [28–30] studied numerically the transient hygrothermal behavior of a hemp concrete building envelope using the simulation environment SPARK. They confirmed that indoor relative humidity variations are more dampened and that the energy consumption is lower when hemp concrete is used in the envelope instead of cellular concrete. Nevertheless, a sensitivity analysis indicates that their results are influenced by the ventilation strategy, by the thermal conductivity or by the presence of wall coating or external layer. At the wall scale, Evrard and De Herde [18,22] focused their work on transient hygrothermal performance of different wall assemblies, starting with determination of hygrothermal material parameters and applying them in WUFI® Pro 4.1 simulations. Hemp concrete assemblies showed a strong ability to improve indoor comfort in comparison to five traditional assemblies with a similar energy consumption of the building. Moreover, they highlighted the influence of the coupled heat and moisture transport phenomena on their results. However, the results of Maalouf and Evrard are not yet validated by experimental data. Such data are rather scarce in the literature, except from the work of Samri [24]. In its work, 1 m² hemp concrete walls (without and with plaster) are placed between a climatic box and the laboratory: one face of the wall is exposed to constant (step functions of time) or cyclic conditions of temperature θ and relative humidity ϕ whereas the other face remains at the uncontrolled conditions of the laboratory. Thereby, Samri measured the hygrothermal response within the material and points out the effect of water phase changes. Nevertheless, numerical simulations based on the Künzle's model and developed in Comsol Multiphysics® do not accurately capture the hygrothermal behavior of its wall: differences may come from uncertainty in the relative humidity measurement within the wall since the embedded sensors were invasive.

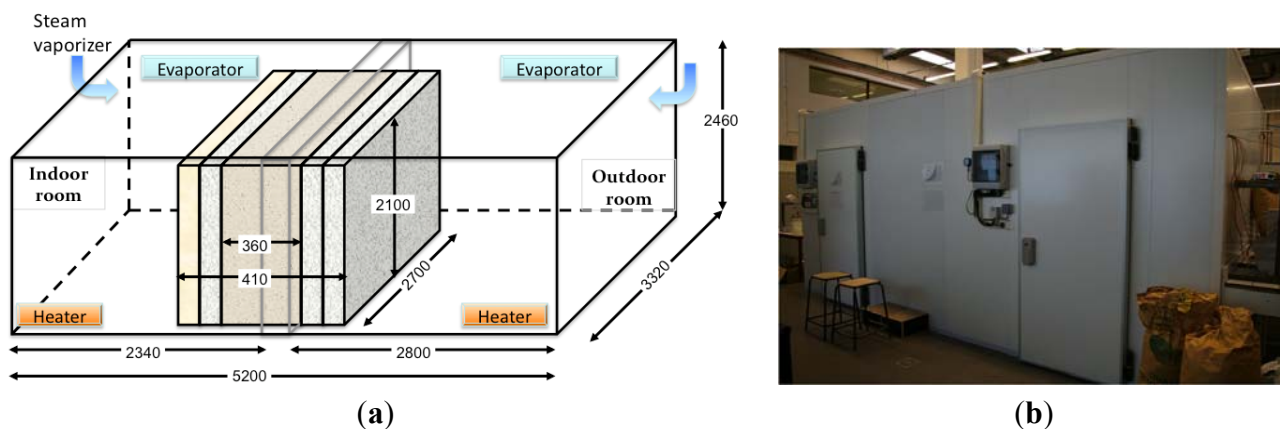
In this work, a specific experimental set-up and methodology is developed in order to investigate the hygrothermal behavior of a sprayed hemp concrete wall. The objective is to complete the previous set of results and to explore experimentally the interactions between the wall and its environment and the significance of the plaster. In this view, Section 2 contains the methods of hygrothermal performance assessment of multilayer hemp concrete wall. Results are presented and discussed in Section 3 before the conclusion.

2. Method of Hygrothermal Behavior Assessment of Multilayer Hemp Concrete Wall

2.1. Experimental Setup: The Biclimate Room and the Hemp Concrete Wall

An experimental apparatus is developed and built at the laboratory of material science at the Université de Bretagne-Sud [31] in order to investigate the hygrothermal behavior of a hemp concrete wall. It consists of three principal components: a specimen support frame and two climatic rooms, one to model indoor climate and the second to model outdoor climate (see Figure 1).

Figure 1. (a) Schematic of the two climatic rooms separated by the hemp concrete wall. (b) Picture of the experimental device.



Each room is insulated from the laboratory with polyurethane panels ($U \approx 0.4 \text{ W}\cdot\text{m}^{-2}\cdot\text{K}^{-1}$) and equipped with heating, refrigeration (for cooling or dehumidifying) and moisture control equipment (steam vaporizer) to maintain temperature and relative humidity to the desired level (see Figure 1a). Controllers (type DR4020 from Eliwell) are used to fix the set points. Working range and accuracy of the set-up are given in Table 1.

Table 1. Working range and accuracy of the two climatic rooms.

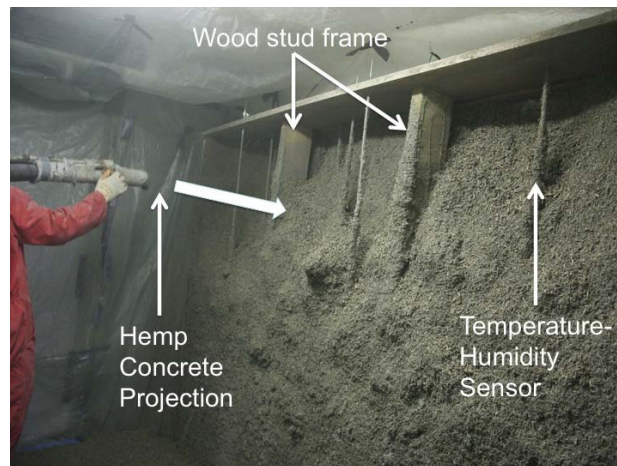
Operating parameter	Room 1 (Indoor)		Room 2 (Outdoor)	
	Range	Accuracy	Range	Accuracy
Temperature θ	18–27 °C	± 0.5 °C	–5–35 °C	± 1 °C
Relative Humidity ϕ	30%–60%	$\pm 2\%$	30%–90%	$\pm 2\%$

The tested material is a hemp concrete wall with dimensions of $270 \times 210 \times 36 \text{ cm}^3$ (length \times height \times thickness). Hemp concrete is prepared according to a wall formulation, defined as 17 wt% of hemp shives (Chanvribat®), 33 wt% of pre-formulated binder (Tradical pf 70®) and 50 wt% of water [21]. Hemp concrete is sprayed on a support with specific concrete spraying machine [20,32]: a dry premix of lime and hemp shives is conducted by air through a hose, and pulverized water is added just before the hose outlet. This setting process has the advantage of providing a continuous homogenous mass and reducing the initial water content within the material, and thus the drying time [20]. In order to correspond to building standards, a wood-stud frame was erected (see Figure 2). Furthermore, the wall is insulated on lateral sides to provide adiabatic boundary conditions, and thus, to ensure one-dimensional heat and moisture flow. Experiments were performed on hemp concrete for two years in order to investigate the drying stage [33] and gain knowledge about its hygrothermal behavior in the view of developing and validating HAM model.

However, in real life, hemp concrete is not used as it is, and plasters are applied on each side in order to correspond to building standards. Permeable and hygroscopic finishes have to be used inside to allow vapor dispersal from the wall, while impermeable coating must be applied outside to protect the wall from the weather load (sun, UV, rain fall, *etc.*). In this view, the interior and exterior coarse plasters are lime-based material and the exterior finishing plaster is a lime sand mixture, whereas the

interior finishing plaster is a lime hemp mixture. Each plaster has a thickness comprised between 1 cm and 2 cm (see Figures 1 and 3).

Figure 2. Wall projection and visualization of the wood-stud frame and the sensors.



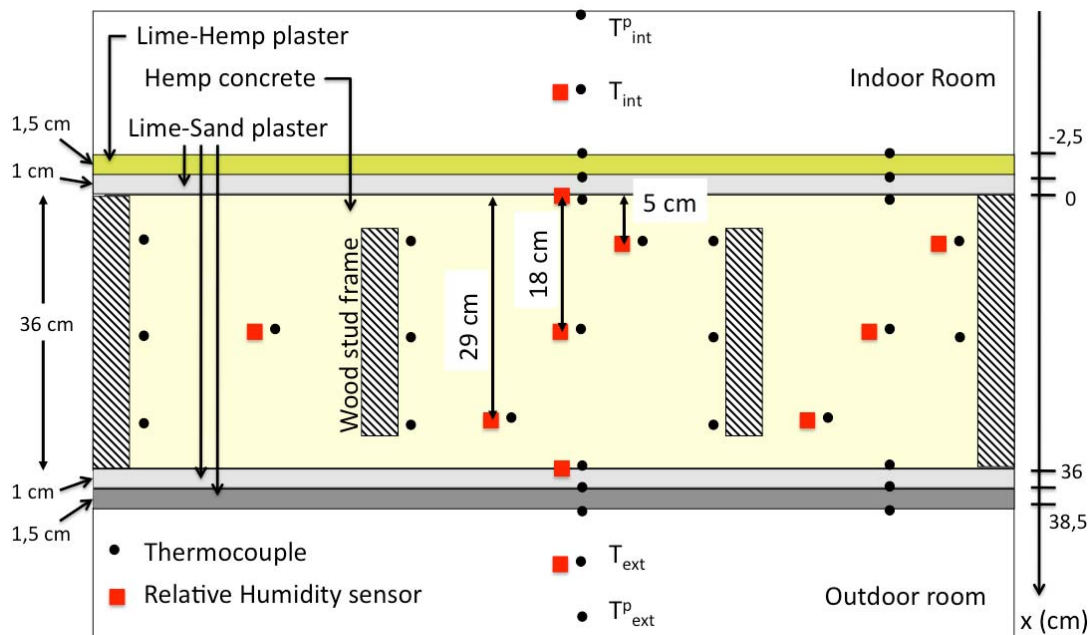
2.2. Monitoring Methods

A monitoring of relative humidity and temperature within the wall is performed with K thermocouples and capacitive humidity sensors (type SHT 75 from Sensirion, measurement range of ϕ from 10% to 90% with an accuracy of $\pm 2\%$ and measurement range of θ from +5 to +45 °C with an accuracy of ± 0.5 °C). The capacitive humidity sensor has a diameter $d = 6$ mm and can thus be inserted inside the sample at different levels without being too much invasive (even inside the plaster). According to the recommendation of Hedenblad [34] on humidity sensor installation (hole drilling and sealing approach), the humidity sensors are inserted within a sealed PVC-tube along the isothermal and iso-humidity lines. For the uncoated wall, humidity sensors are placed close to the indoor and outdoor rooms (resp. at $x = 5$ cm and $x = 29$ cm) and in the center of the wall. For the coated wall, additional humidity sensors are placed at the interfaces between the wall and the plasters.

Surface temperatures of the tested wall and of the room panels are measured with K thermocouples and selectively confirmed with optical pyrometers. Air temperature and relative humidity are measured in the center of each room with a thermocouple placed inside radiation shield and two capacitive humidity sensors (type HC2-S from Rotronic and type SHT 75 from Sensirion). Finally, additional sensors are selectively employed to investigate the stratification and evaluate the air velocity within the room. The positioning of all sensors is shown in Figure 3.

A data logger reads all sensor signals and the measured values are then sent to a computer where they are stored. All data are recorded every 10 min during the experiment.

Figure 3. Localisation of temperature and relative humidity sensors within the coated hemp concrete wall.



2.3. Experimental Procedure

The biclimatic room test facility allows us to:

- Evaluate temperature and relative humidity in time and in space,
- Examine the drying stage of sprayed hemp concrete [33],
- Characterize the hygrothermal behavior of hemp concrete as function of boundary conditions,
- Investigate the influence of plasters on the hygrothermal performances of the wall.

Consequently, a series of experiments have been conducted to gather data that quantify heat, air and moisture (HAM) transport within the uncoated and coated hemp concrete wall. One of the objectives is to collect data of simple experiments (but not necessarily representative of climatic load) that are suited to benchmark detailed numerical models.

Since the hygrothermal performance of a building envelope system is dictated by the response of the system to combined heat, air and moisture fluctuations produced by exterior and interior conditions that exist on either side of the envelope, the following strategy has been adopted: indoor conditions are controlled (contrary to the work of Samri [24]) and kept constant at 23 °C and 50% relative humidity whereas outdoor conditions are incrementally changed to create temperature and/or relative humidity gradients. Table 2 summarizes the room conditions and the measurement strategy used.

In Table 2, the vapor pressure p_v is calculated from the temperature T (in K) and the relative humidity ϕ (in %) as:

$$p_v = \frac{\phi}{100} * 133.33 * \exp\left(46.784 - \frac{6435}{T} - 3.868 * \ln(T)\right) \quad (1)$$

Table 2. Measurement strategy for non-isothermal, steady-state measurements.

Operating parameter		θ [°C]	ϕ [%]	P_v [Pa]
Indoor conditions		23	50	1400
	Experiment 1	23 → 32	50 → 30	1400
Outdoor conditions	Experiment 2	23 → 32	50	1400 → 2360
	Experiment 3	32	50 → 30	2360 → 1400

2.4. Thermal Model

2.4.1. Heat Transfer Model

To enhance the understanding and interpretation of the experimental data, a conductive thermal model is used for evaluating the thermal behavior of the hemp concrete wall. Here, a macroscopic description is adopted even though the materials present heterogeneous and anisotropic microstructures [25]. Convection, moisture transfer and associated latent heat transfer across the wall are not considered in this work. Finally, heat transfers are solved far from the wood-stud frame (*i.e.*, in the homogeneous part of the wall), and can thus be considered as one-dimensional. Heat transfers in the wall layer noted i are given by:

$$\rho_{bi} c_{pi} \frac{\partial T_i(x,t)}{\partial t} = \lambda_{effi} \frac{\partial^2 T_i(x,t)}{\partial x^2} \text{ for } 1 \leq i \leq N \quad (2)$$

where $\rho_{bi} c_{pi}$ is the apparent volumetric heat capacity; λ_{effi} the effective thermal conductivity; and T_i the temperature in the layer I ; N is the number of layer: $N = 1$ for the uncoated wall; $N = 5$ for the coated wall. In the case of the coated wall, a perfect thermal contact between each layer is assumed, which implies a continuity of temperatures and heat flows at each interface.

2.4.2. Boundary and Initial Conditions

For the uncoated and coated wall, convective and radiative boundary conditions are considered:

$$-\lambda_1 \frac{\partial T_1(x,t)}{\partial x} = h_{int} (T_{int} - T_1) + \varepsilon_1 \sigma (T_{int}^{P4} - T_1^4) \quad (3)$$

$$-\lambda_N \frac{\partial T_N(x,t)}{\partial x} = h_{ext} (T_{ext} - T_N) + \varepsilon_N \sigma (T_{ext}^{P4} - T_N^4) \quad (4)$$

where h_{int} (resp. h_{ext}) is the convective transfer coefficients at the inner (resp. outer) surfaces; ε_1 (resp. ε_N) the emissivity of the inner (resp. outer) surface, *i.e.*, hemp concrete for the uncoated and lime-hemp plaster the coated wall (resp. hemp concrete or lime-sand plaster). Indoor and outdoor air (T_{int} and T_{ext}) and room panels (T_{int}^P and T_{ext}^P) temperature are those measured by the sensors.

Initial conditions within the wall are given by the point measurements and are extrapolated over the wall thickness. The numerical model was developed in the Comsol Multiphysics® environment.

3. Results and Discussion

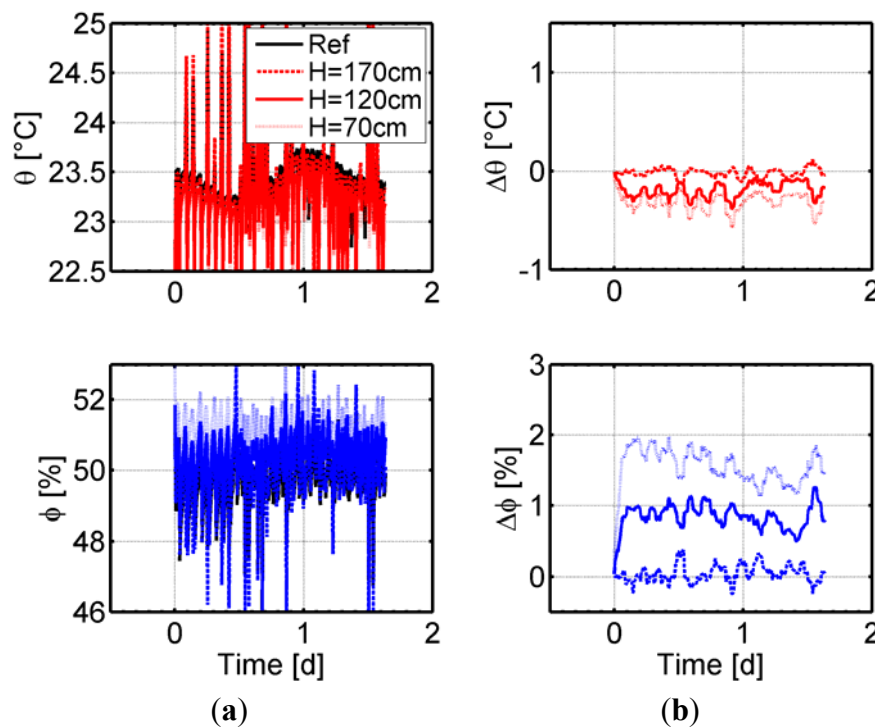
3.1. Hygrothermal Behavior of Uncoated Hemp Concrete

Results for a monolayer hemp concrete wall are extensively described in the next section. First, the experimental results should confirm the performance and the repeatability of the newly developed test set-up, validate the measurement methodology and provide trends in the hygrothermal behavior of hemp concrete. Then, a comparison with the numerical model is proposed.

3.1.1. Evaluation of Boundary Conditions

Before analyzing any results, boundary conditions are first evaluated. Every test should be carried out under well-mixed air conditions and under almost uniform temperature and relative humidity inside the climatic chambers. In this view, measurements of θ and ϕ are performed at eight different positions within the rooms and directly compared with those obtained with the reference sensor located at the center of the rooms. For example, Figure 4 shows the evolution of θ and ϕ at different heights in the indoor room (left graphs) and their variations compared to the reference sensor (right graphs): the differences are less than $0.5\text{ }^{\circ}\text{C}$ and 2%, *i.e.*, within the accuracy range of the sensors. It confirms that there are obviously no temperature stratification and no uneven moisture distribution within rooms. Thus, one sensor at the center of each test room may well catch the variations of θ and ϕ in the room.

Figure 4. θ and ϕ within the indoor room measured at different heights (a) and comparison to the reference sensor located in the center of the room (b).



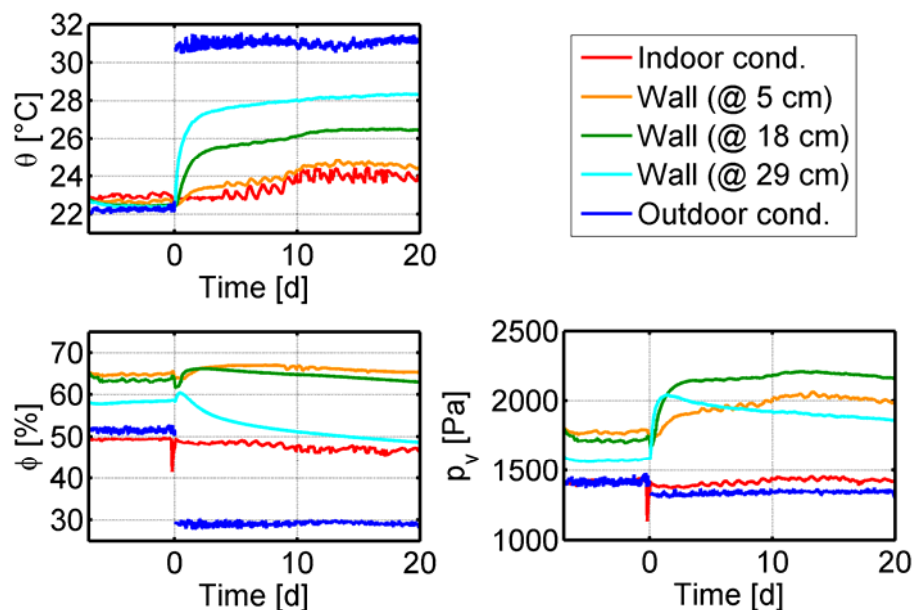
Additional air velocity measurements were performed at different locations within the room. Air velocity reaches a maximum value of $1.5\text{ m}\cdot\text{s}^{-1}$ at the evaporator outlet, but does not exceed $0.2\text{ m}\cdot\text{s}^{-1}$ close to the tested wall. Consequently, natural convection may be prevalent within both rooms.

3.1.2. Experimental Response to a Temperature and Relative Humidity Gradient (Experiment 1)

Experiment 1 consists in applying a temperature gradient and in maintaining the vapor pressure constant through the wall (see Table 2): θ_{ext} increases from 23 °C to 32 °C, ϕ_{ext} decreases from 50% to 30%, so that $p_{v\text{-ext}}$ is maintained at 1400 Pa. Indoor conditions are kept constant throughout the experiment. Before changing the set points, the wall was conditioned during 100 days and the experiment lasted 45 days.

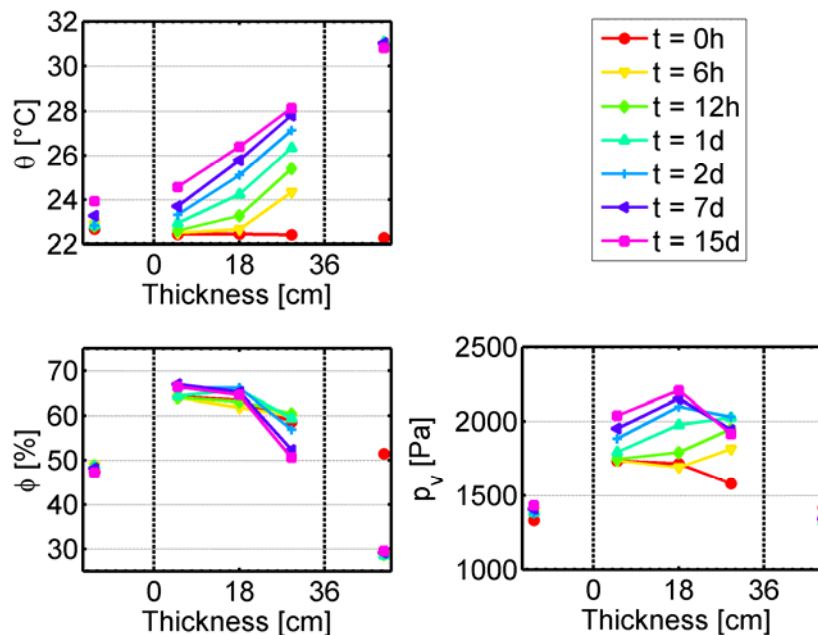
Figure 5 presents the temporal variations of θ , ϕ and p_v , respectively, in both climatic rooms and at three positions within the wall (see Figure 3): close to the indoor ($x = 5$ cm) and the outdoor room ($x = 29$ cm) and in the wall center ($x = 18$ cm). First, we note that temperature and relative humidity set points are rapidly reached within the rooms. As expected, the thermal response of the wall is faster than the hygric response. The closer to the exterior, the higher the amplitude is and the shorter the delay in the temperature response is. The thermal steady state is reached in less than 7 days. Concerning relative humidity, only the sensor at $x = 29$ cm is influenced by the change in the set points, while the other two remain almost constant. Because of θ and ϕ variations, the vapor pressure varies fast over the thickness at the beginning, and decrease then slowly at $x = 29$ cm.

Figure 5. Time response in θ , ϕ and p_v at $x = 5, 18$ and 29 cm of uncoated hemp concrete wall subjected to temperature and relative humidity gradient.



Looking at the profiles measured at different times shown in Figure 6, we observe that temperature close to the indoor room ($x = 5$ cm) has not changed over 15 days whereas temperature in the wall center ($x = 18$ cm) starts to increase only 12 hours after the change in the set points, indicating that hemp concrete may provide a good thermal inertia to the building envelope. At steady state ($t = 15$ d), as expected, temperature presents a linear profile. Relative humidity profile remains almost unchanged during the experiment.

Figure 6. Spatial response in θ , ϕ and p_v at $t = 0, 0.25, 0.5, 1, 2, 7$ and 15 days of uncoated hemp concrete wall subjected to temperature and relative humidity gradient.



On the other hand, the vapor pressure increases during the first days ($t < 5$ d) on the outdoor side ($x = 29$ cm): this may be attributed to evaporation and molecular desorption. Indeed, for given temperature and relative humidity, capillary condensation occurs in pore with a radius r given by the Kelvin-Laplace equation:

$$r = \frac{-2\sigma \cos \vartheta}{\rho_l \frac{RT}{M_w} \ln(\phi)} \quad (5)$$

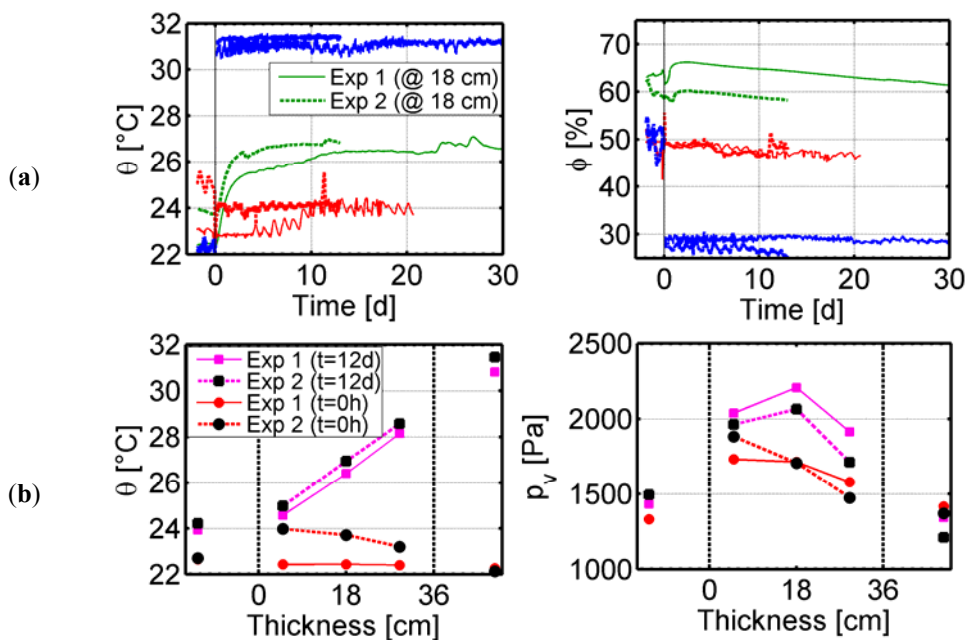
Where σ is the surface tension; ϑ is the contact angle; ρ_l is the liquid water density; M_w the water molecular weight; and R is the gas constant.

Consequently, for increasing T and constant ϕ , capillary condensation occurs in smaller pores: part of water molecules contained in larger pores is thus released in the porous structure and p_v increases (at this point, instantaneous hemp concrete moisture content is supposed to be constant). Then, as a vapor pressure gradient exists between the wall and the chambers, vapor transfer should take place. Nevertheless, as hemp concrete exhibits a high water vapor resistance factor [23], vapor diffusion occurs very slowly and the vapor pressure level is lightly reduced on the outdoor side (at this point, hemp concrete moisture content has decreased with increasing temperature, which is consistent with the literature on sorption of hygroscopic materials). After 15 days, vapor pressure within the wall has not reached the steady state and is still higher than the boundary condition, indicating that the moisture contained in the wall could condensate if the temperature should decrease.

Finally, even if this particular set of measurements could theoretically identify a moisture flux under a temperature gradient in the absence of a vapor pressure gradient, any thermodiffusive effect, independent of temperature generated vapor pressure gradients, is practically immeasurable.

Experiment 1 has been repeated once to validate the previous observations. Transient evolutions of θ and ϕ are shown on the top graphs of Figure 7. First, we observe that the outdoor conditions are well repeated. Small deviations exist in the transient response of the temperature and the relative humidity at the wall center ($x = 18$ cm), but it comes from different initial conditions. Bottom graphs of Figure 7 present the initial and final ($t = 12$ d) temperature and vapor pressure profiles. Final temperature profiles of the two distinct experiments are well overlaid while the vapor pressure profiles exhibit a small difference that remains in the order of measurement's confidence. These results confirm the good reproducibility of the experiments.

Figure 7. Repeatability of the Experiment 1: (a) time response in θ and ϕ at $x = 18$ cm; and (b) spatial response in θ and p_v at $t = 0$ and 12 d of uncoated hemp concrete wall subjected to temperature and relative humidity gradient. (Solid lines refer to the first experiment, dashed line to the second experiment).



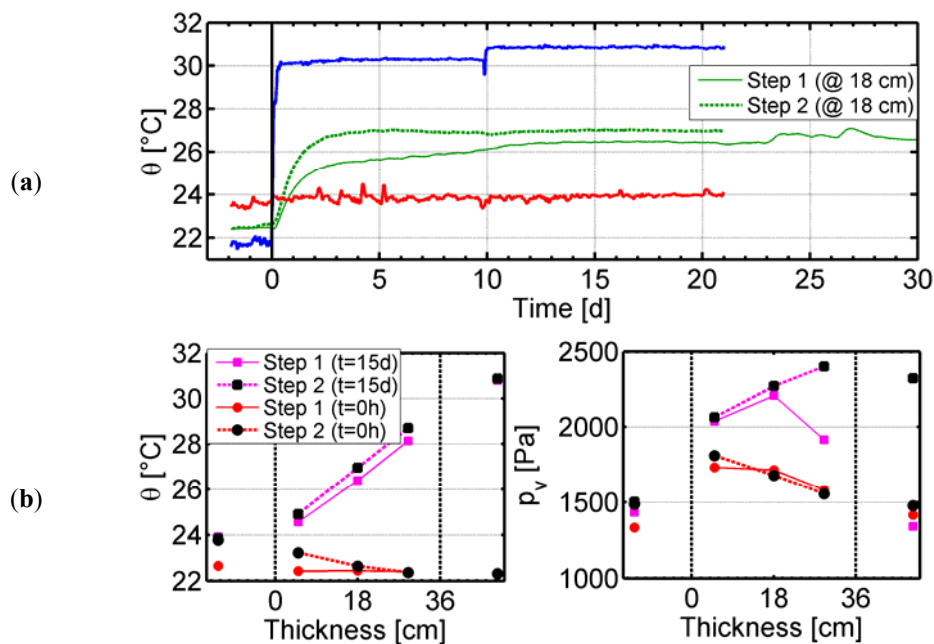
3.1.3. Experimental Response to a Temperature and Vapor Pressure Gradient (Experiments 2 and 3)

In this section, Experiments 2 and 3 are performed on the uncoated hemp concrete wall and directly compared with Experiment 1 (see Table 2). Results are presented successively in Figures 8 and 9. For clarity, only the temperature variations at the wall center ($x = 18$ cm) and the initial ($t = 0$ d) and final ($t = 15$ d) profiles are shown.

Figure 8 allows investigating the transient and steady state responses of the wall when a temperature gradient is associated with or without a vapor pressure gradient. First, we note for both experiments that initial conditions are the same, transient evolution of the temperature at the wall center is found to be similar and steady state is reached rapidly (top graph). However, the temperature level at the wall center and more generally the slope of the temperature profile (left bottom graph) are higher for steady state when ϕ is constant. Concerning the vapor pressure (right bottom graph), differences are only observed close to the outdoor room ($x = 29$ cm). At this position, hemp concrete moisture content should decrease more for Experiment 1 than for Experiment 2 since θ increases and ϕ

decreases. Therefore, the amount of evaporated water should be higher and a part of the energy is transferred as latent heat. Consequently, sensible heat transfer through the wall is more limited and could explain the lower temperature increase at the wall center in case of Experiment 1.

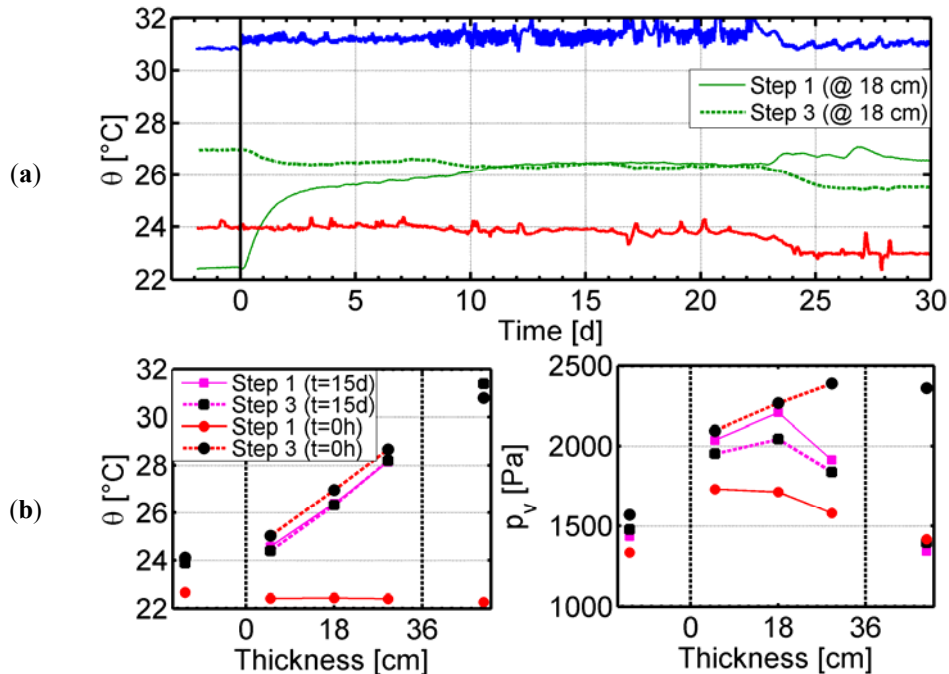
Figure 8. (a) Time response in θ at $x = 18$ cm; and (b) spatial response in θ and p_v at $t = 0$ and 15 d of uncoated hemp concrete wall subjected to Experiment 1 (solid lines) and Experiment 2 (dashed lines).



However, these experiments cannot conclude on the moisture flow through hemp concrete. Indeed, Peuhkuri *et al.* [35] examined similar non-isothermal moisture transport and highlighted the following contradiction: the moisture content is usually higher on the cold side of building envelopes, driving the moisture from cold to warm. Nevertheless, the use of the simplest models with only water vapor diffusion will result in a gradient of absorbed moisture content within a porous, water-absorbent material, which will tend to drive water in the opposite direction.

As the final set points of experiment 1 and 3 are the same, Figure 9 allows investigating the influence of the initial conditions on the transient and steady state responses of the wall. As shown on the bottom graphs, temperature profiles are strictly the same as for steady state, while relative humidity and vapor pressure profiles are similar to the measurement uncertainty. This indicates that long-term response of hemp concrete wall does not depend on initial state. Moreover, the analysis of transient response indicates that the temperature decreases at the wall center during the first two days and remains constant after (top graph). This observation can be attributed to the evaporation. Indeed, as vapor pressure is reduced in the outdoor room, vapor transport should take place from the higher potential to the lower, thus simultaneously reducing the vapor pressure and relative humidity levels within the material. Consequently, hemp concrete moisture content should lightly decrease: condensed pore water is vaporized and temperature decreases locally.

Figure 9. (a) Time response in θ at the wall center; (b) and spatial response in θ and p_v of uncoated hemp concrete wall subjected to Experiment 1 (solid lines) and Experiment 3 (dashed lines).



3.1.4. Comparison with Numerical Results

Measured temperatures are compared to numerical ones in Figures 10–12. Even if hemp concrete thermal conductivity increases with increasing temperature θ and relative humidity ϕ [25], we observe that similar values of thermal conductivity were found at (23 °C, 50%) and at (32 °C, 30%), thus a constant value of $0.1 \text{ W}\cdot\text{m}^{-1}\cdot\text{K}^{-1}$ is used for simulation. Similarly, thermal diffusivity is set at $2\times 10^{-7} \text{ m}^2\cdot\text{s}^{-1}$. Since air velocity do not exceed $0.2 \text{ m}\cdot\text{s}^{-1}$ close to the wall surface, convective transfer coefficients are calculated for free convection at a vertical wall as [36]:

$$h = \frac{\lambda_a}{H} 0.025 Ra^{0.4} \quad (6)$$

where λ_a is the air thermal conductivity; H the height of the wall and Ra the Rayleigh number.

For the experimental conditions, values around $2 \text{ W}\cdot\text{m}^{-2}\cdot\text{K}^{-1}$ are found. Since uncertainty exists in the thermal conductivity (depending on the measurement method) and in the convective transfer coefficients, a sensitivity analysis is carried out. Investigated parameters are presented in Table 3. Finally, no values of the hemp concrete emissivity are available in the literature. However, since most of building materials have an emissivity of $0.8 < \varepsilon < 0.95$, a value of 0.9 may be acceptable. Furthermore, a sensitivity analysis not presented in this work indicates that this parameter has no influence on the simulated temperature variations.

Table 3. Parameters used for the sensitivity analysis.

Parameters	h ($\text{W}\cdot\text{m}^{-2}\cdot\text{K}^{-1}$)	λ ($\text{W}\cdot\text{m}^{-1}\cdot\text{K}^{-1}$)	a ($10^{-7} \text{m}^2\cdot\text{s}^{-1}$)
Parameter 1	2	0.1	2
Parameter 2	5	0.1	2
Parameter 3	2	0.13	2.5
Parameter 4	5	0.13	2.5

Experimental (from Experiment 1) and numerical temperature profiles presented on top graph of Figure 10 show a good agreement at steady state. Although latent heat transfer associated with moisture transfer is not accounted for in the simulation, a similarity between experimental and numerical transient temperatures is observed on bottom graph of Figure 10. Nevertheless, predicted temperatures are still higher than the experimental ones during the first days, specifically for temperatures close to the outdoor room ($x = 29$ cm). In fact, heat is transferred in the form of sensible heat (as described by the thermal model) and of latent heat, causing the evaporation of water until new hygric equilibrium is reached. For this experiment, the equilibrium seems to be reached after 12 days.

Results of the sensitivity analysis are shown at $t = 15$ d and at $x = 18$ cm in Figure 11. Increasing the convective transfer coefficients leads to higher temperature levels within the wall, while increasing the thermal conductivity and diffusivity has almost no influence in the present case.

Figure 10. Comparison between experimental (black lines) and simulated (colored lines) temperature of uncoated hemp concrete wall subjected to Experiment 1. Top graph (a) shows the spatial response at $t = 0$ and 15 d; bottom graph (b) shows the transient response at $x = 5, 18$ and 29 cm.

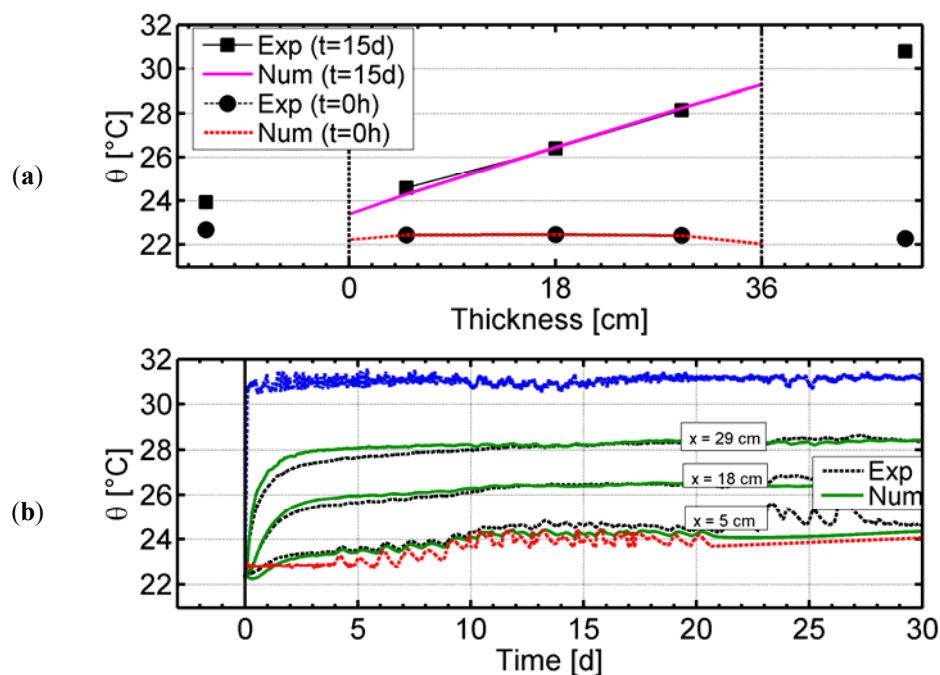
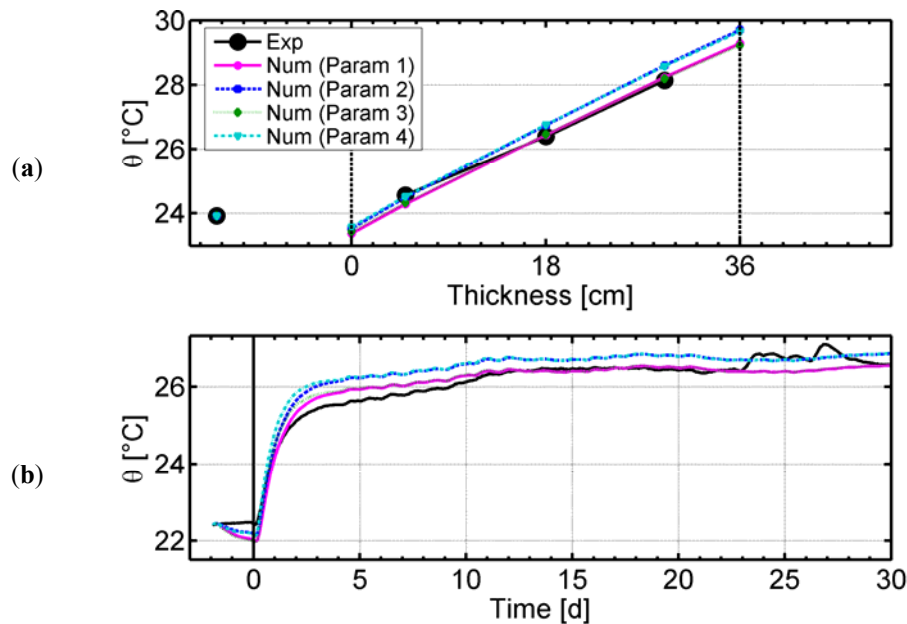
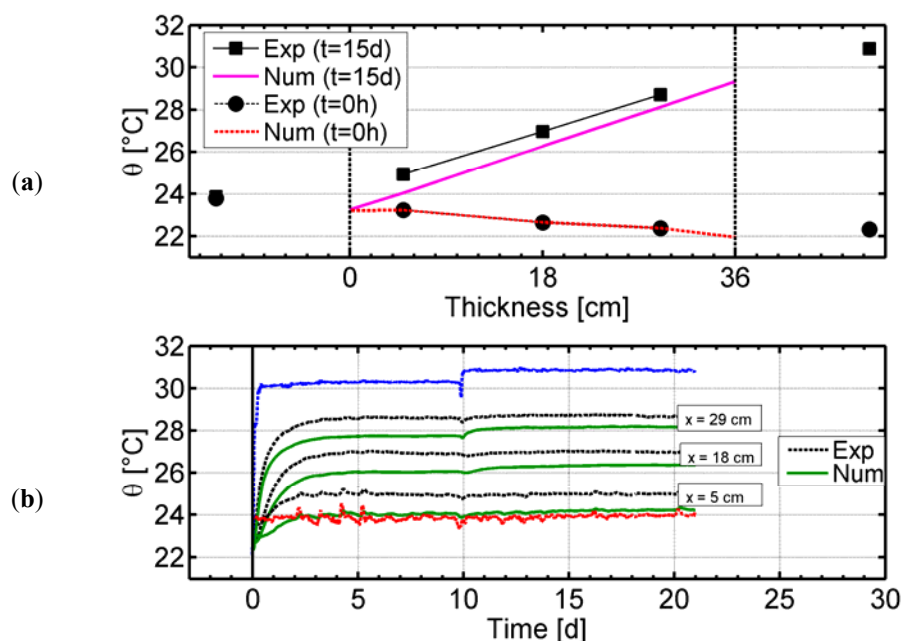


Figure 11. Sensitivity analysis (colored lines) to the thermal properties (see Table 3) and comparison to experimental results (black lines). Top graph (a) shows the spatial response at $t = 15$ d; bottom graph (b) the transient response at $x = 18$ cm.



Finally, numerical and experimental results of Experiment 2 are presented in Figure 12. Globally, we observe that the numerical results are also lower than the experimental ones, but profiles at steady state are parallel.

Figure 12. Comparison between experimental (black lines) and simulated (colored lines) temperature of uncoated hemp concrete wall subjected to Experiment 2. Top graph (a) shows the spatial response at $t = 0$ and 15 d; bottom graph (b) the transient response at $x = 5, 18$ and 29 cm.



3.2. Hygrothermal Behavior of Coated Hemp Concrete

In this section, we investigate the effect of plastering on the hygrothermal behavior of a hemp concrete wall by applying the same boundary conditions as on the uncoated wall. Results are presented in Figures 13–15.

3.2.1. Experimental Response to a Temperature and Relative Humidity Gradient

Figure 13 presents a comparison of transient temperature and steady state ($t = 8$ d) temperature and vapor pressure profile for coated and uncoated wall subjected to a temperature and relative humidity gradient. First, we observe that temperature profiles are similar for steady state and transient state. Only a small time delay is observed in the temperature response in the presence of plasters. These light differences come from the small thickness of the plasters (1 to 2 cm) and their low thermal resistance. On the other hand, vapor pressure levels are lower within the wall when plasters are applied. It comes from the fact that plasters are less permeable to vapor [23] and thus act as barrier for vapor diffusion. Finally, we observe that even if vapor pressure levels are not exactly the same, the difference between initial and final state are similar. Thus, the amount of vaporized water is the same for coated and uncoated wall, and consequently, the presence of plaster does not affect the evaporation phenomena within hemp concrete.

Figure 13. Comparison of experimental results for uncoated (solid lines) and coated (dashed lines) wall subjected to temperature and relative humidity gradient. Time response in θ is shown on the top graph (a); and spatial response in θ and p_v of hemp concrete wall is shown on the bottom graph (b).

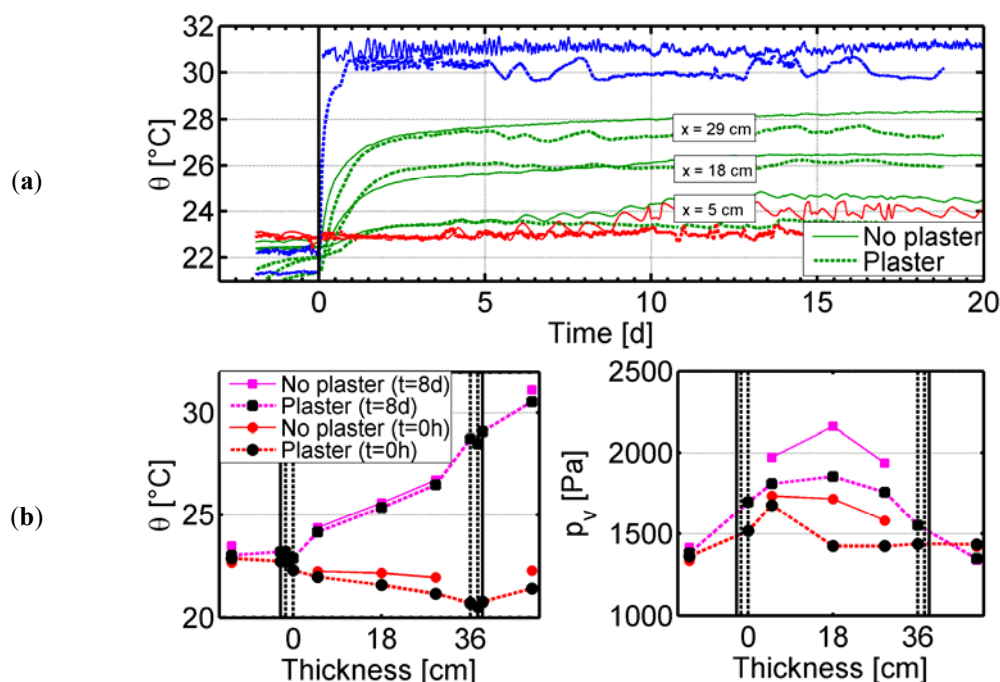


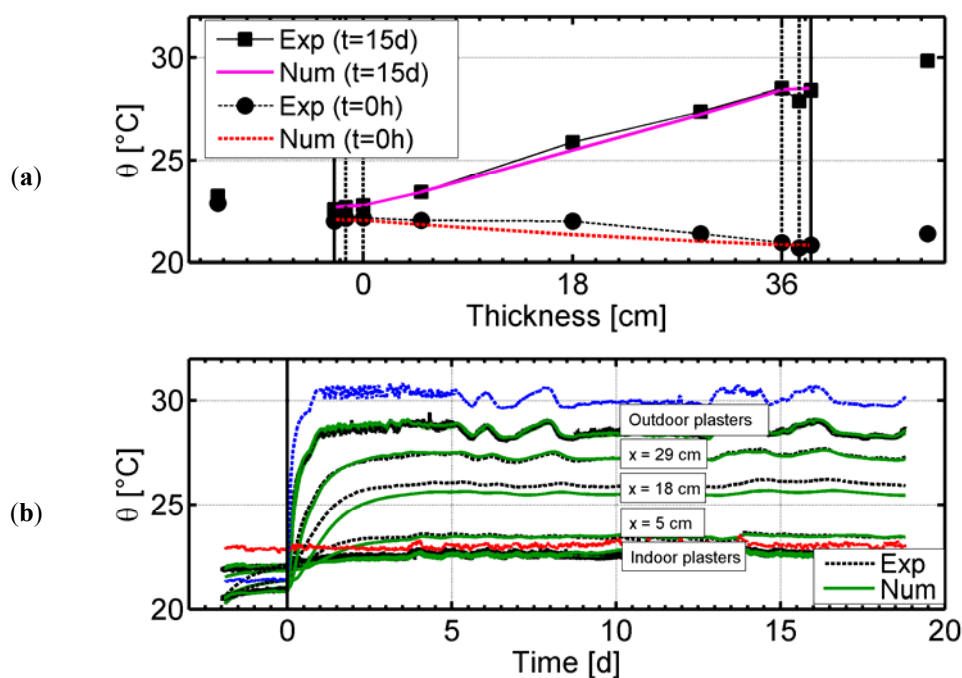
Figure 14 allows comparing experimental and numerical results. Thermal properties used for the simulation are summarized on Table 4. As in Figure 10, the steady state temperature profiles overlay perfectly. Transient evolution of temperature is also well caught, even for the indoor and the outdoor

plaster. Only a small difference can be observed at the wall center. We note in Figure 14 that indoor plaster temperature levels are lower than the indoor air temperature.

Table 4. Thermal properties of hemp concrete and plasters used for simulation.

Material	Density ($\text{kg}\cdot\text{m}^{-3}$)	Thermal conductivity ($\text{W}\cdot\text{m}^{-1}\cdot\text{K}^{-1}$)	Thermal diffusivity ($10^{-7} \text{ m}^2\cdot\text{s}^{-1}$)
Lime-Hemp plaster (interior finishing plaster)	990	0.23	2.41
Lime-Sand plaster (interior coarse plaster)	1660	0.58	4.31
Hemp concrete	440	0.1	2.00
Lime-Sand plaster (exterior coarse plaster)	1590	0.39	3.03
Lime-Sand plaster (exterior finishing plaster)	1600	0.39	2.94

Figure 14. Comparison between experimental (black lines) and simulated (colored lines) temperature of coated hemp concrete wall subjected to temperature and relative humidity gradient. (a) Top graph shows the spatial response at $t = 0$ and 15 d; (b) bottom graph the transient response at $x = 5, 18$ and 29 cm.

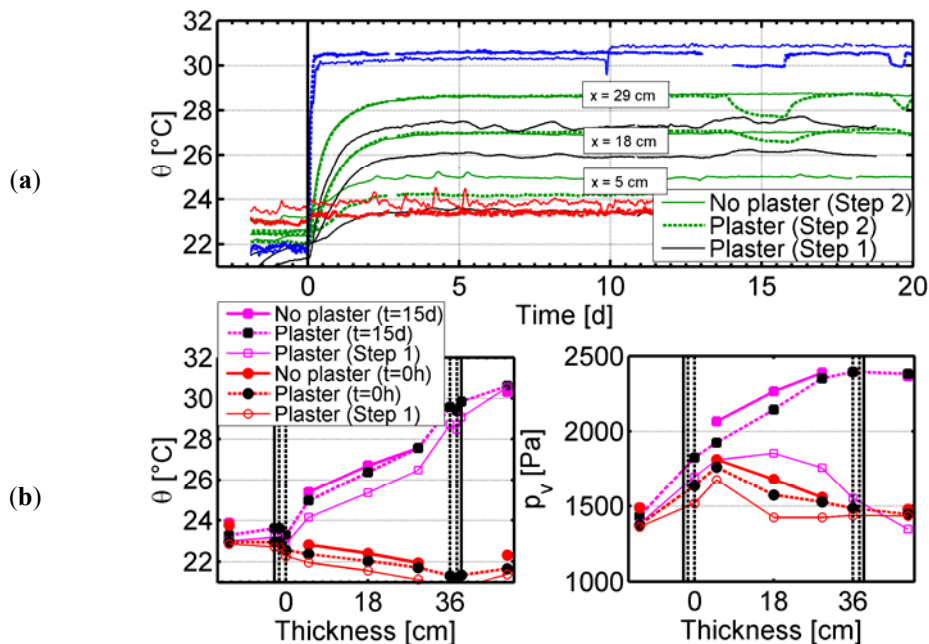


3.2.2. Experimental Response to a Temperature and Vapor Pressure Gradient

Figure 15 shows the experimental results for the uncoated and the coated wall when vapor pressure gradient is applied in addition to the temperature gradient (Experiment 2). For comparison, results of Experiment 1 for the coated wall are also plotted. Initially, temperature and vapor pressure profiles are similar. Once again, temperature increase at the wall center is not influenced by the presence of

plasters whereas a difference is still observed between the two experiments as for the uncoated wall (top graph). At steady state, temperature and vapor pressure profiles are very similar (bottom graphs).

Figure 15. Comparison of experimental results for uncoated (solid lines) and coated (dashed lines) wall subjected to temperature and vapor pressure gradient. Time response in θ is shown on the top graph (a); and spatial response in θ and p_v of hemp concrete wall is shown on the bottom graph (b).



On the other hand, temperatures in the indoor plasters are always lower than indoor temperature, indicating that an endothermic phenomenon may exist in addition to the radiative heat transfer. At this interface, relative humidity is around 50% and a vapor pressure gradient is established through the wall (bottom right graph). Lime-hemp plaster presents a monomodal pore size distribution [23], with a main peak at about $0.9 \mu\text{m}$ and a secondary peak at about $0.075 \mu\text{m}$ for which capillary condensation occurs when $\phi < 50\%$ according to equation (5): liquid water may exist in the indoor plaster. Moreover, Fick's law indicates that vapor pressure gradient implies a moisture transport from outdoor to indoor side, even within the indoor plasters. Consequently, evaporation is probably the phenomenon that reduces the temperature on the indoor side of the wall. These observed phenomena could be assimilated to a "cold wall effect" during summer period and therefore insure a better thermal comfort. On the other hand, these phenomena were not observed for the uncoated wall since the number of micropores within hemp concrete is lower and thus there is less liquid water: moisture transfer within the uncoated wall occurs without evaporation on the surface and temperature profile is not modified.

Results for Experiment 3 are not presented, but the trend is similar as for the uncoated wall (see Figure 9): the temperature decreases lightly at the wall center (because of the evaporation) when the relative humidity is reduced while a temperature gradient is still applied. Moreover, the final profile of temperature and vapor pressure does not depend on the initial profiles, when similar climatic loads are applied. Finally, the vapor pressure presents a parabolic profile at steady state, whether the wall is coated or not.

4. Conclusions

Hemp concrete buildings are still at a pioneer stage and still require many more efforts to gain knowledge on its transient hygrothermal behavior. In this view, a large-scale experimental device has been set up in order to control the indoor and outdoor boundary conditions around a hemp concrete wall. Well-defined temperature and/or vapor pressure gradient are applied first through an uncoated hemp concrete wall, and then through a wall coated with lime-hemp and lime-sand plasters. Experiments on the uncoated wall allow validating the method (repeatability/reliability of the measurement) and could point out water phase change. Moreover, it was shown that a single thermal model could reproduce the thermal behavior of the wall for some boundary conditions. When plasters are applied, heat transfers are almost not modified since plasters have a lower thermal resistance than hemp concrete. On the other hand, moisture transfers are modified since plasters are less permeable than hemp concrete and vapor pressure levels are more dampened for the coated wall. Evaporation phenomena were also experimentally observed at the interior surface for summer conditions. Moreover, the non-isothermal tests show that the vapor pressure gradient seems to be the most important driving potential for moisture transfer within hemp concrete. Finally, these simple experiments could help in the understanding of transfer and storage mechanisms within hemp concrete and could serve to validate a heat and moisture transfer model.

Acknowledgments

The authors want to thank the Brittany Regional Council (Region Bretagne) and the National Research Agency of France (ANR) for their financial contributions.

References

1. Osanyintola, O.F.; Simonson, C.J. Moisture buffering capacity of hygroscopic building materials: Experimental facilities and energy impact. *Energy Build.* **2006**, *38*, 1270–1282.
2. Steeman, M.; Janssens, A.; De Paepe, M. Performance evaluation of indirect evaporative cooling using whole-building hygrothermal simulations. *Appl. Therm. Eng.* **2009**, *29*, 2870–2875.
3. Woloszyn, M.; Kalamees, T.; Abadie, M.O.; Steeman, M.; Kalagsidis, S.A. The effect of combining a relative-humidity-sensitive ventilation system with the moisture-buffering capacity of materials on indoor climate and energy efficiency of buildings. *Build. Environ.* **2009**, *44*, 515–524.
4. Simonson, C.J.; Salonvaara, M.; Ojanen, T. The effects of structures on indoor humidity—Possibility to improve comfort and perceived air quality. *Indoor Air* **2002**, *12*, 243–251.
5. El Diasty, R.; Fazio, P.; Budaiwi, I. Modelling of indoor air humidity: The dynamic behavior within an enclosure. *Energy Build.* **1992**, *19*, 61–73.
6. Woloszyn, M.; Rode, C. Tools for performance simulation of heat, air and moisture conditions of whole buildings. *Build. Simul.* **2008**, *1*, 5–24.
7. Hagentoft, C.E.; Kalagasidis, S.A.; Adl-Zarrabi, B.; Roels, S.; Carmeliet, J.; Hens, H.; Grunewald, J.; Funk, M.; Becker, R.; Shamir, D.; Adan, O.; Brocken, H.; Kumaran, K.; Djebbar, R. Assessment method of numerical prediction models for combined heat, air and moisture transfer in building components: Benchmarks for one-dimensional cases. *J. Therm. Env. Build. Sci.* **2004**, *27*, 327–352.

8. Hagentoft, C.E. Heat, air and moisture transfer through new and retrofitted insulated envelope parts. Task 5: Performances and practice. In *Final Report of IEA Annex 24*; Katholieke Universiteit Leuven: Leuven, Belgium, 1998.
9. Van Belleghem, M.; Steeman, M.; Willockx, A.; Janssens, A.; De Paepe, M. Benchmark experiments for moisture transfer modelling in air and porous materials. *Build. Environ.* **2011**, *46*, 884–898.
10. Carmeliet, J.; Derome, D. Temperature driven inward vapor diffusion under constant and cyclic loading in small-scale wall assemblies: Part 1 experimental investigation. *Build. Environ.* **2012**, *48*, 48–56.
11. Rode, C.; Salonvaara, M.; Ojanen, T.; Simonson, C.; Grau, K. Integrated hygrothermal analysis of ecological buildings. In *Proceedings of the 2nd International Building Physics Conference*, Leuven, Belgium, 14 September 2003.
12. Pavlik, Z.; Cerny, R. Hygrothermal performance study of an innovative interior thermal insulation system. *Appl. Therm. Eng.* **2009**, *29*, 1941–1946.
13. Kalamees, T.; Vinha, J. Hygrothermal calculations and laboratory tests on timber-framed wall structures. *Build. Environ.* **2003**, *38*, 689–697.
14. Belarbi, R.; Qin, M.; Aït-Mokhtar, A.; Nilsson, L.O. Experimental and theoretical investigation of non-isothermal transfer in hygroscopic building materials. *Build. Environ.* **2008**, *43*, 2154–2162.
15. Yang, X.; Vera, S.; Rao, J.; Ge, H.; Fazio, P. Full-scale experimental investigation of moisture buffering effect and indoor moisture distribution. In *Proceedings of the Building X Conference*, Clearwater Beach, FL, USA, 2–7 December 2007.
16. Woolley, T.; Thompson, H.; McGrogan, T.; Alexander, M. The role of low impact building materials in sustainable construction: The potential for hemp. In *Proceedings of the Sustainable Building Conference*, Stellenbosch, South Africa, 13–18 September 2004.
17. Bevan, R.; Woolley, T. *Hemp Lime Construction: A Guide to Building with Hemp Lime Composites*; IHS/BRE Press: Bracknell, Berkshire, UK, 2008.
18. Evrard, A.; De Herde, A. Hygrothermal performance of lime-hemp wall assemblies. *J. Build. Phys.* **2010**, *34*, 5–25.
19. Garnier, C.; Pretot, S.; Collet, F. Life cycle assessment of a hemp concrete wall manufactured by spraying. In *Proceedings of The Second International Conference on Building Energy and Environment*, Boulder, CO, USA, 1–4 August 2012.
20. Colinart, T.; Glouannec, P.; Chauvelon, P. Influence of the setting process and the formulation on the drying of hemp concrete. *Constr. Build. Mater.* **2012**, *30*, 372–380.
21. Cerezo, V. Propriétés Mécaniques, Thermiques et Acoustiques d'un Matériau à Base de Particules Végétales: Approche Expérimentale et Modélisation Théorique (in French). Ph.D. Dissertation, ENTPE (Ecole Nationale des Travaux publics de l'Etat), Lyon, France, 16 June 2005.
22. Evrard, A. Transient Hygrothermal Behavior of Lime-Hemp Materials. Ph.D. Dissertation, Université Catholique de Louvain, Louvain, Belgium, 5 March 2008.
23. Collet, F. Caractérisation Hydrique et Thermique de Matériaux de Génie Civil à Faibles Impacts Environnementaux (in French). Ph.D. Dissertation, INSA (The Institut National des Sciences Appliquées), Rennes, France, 14 December 2004.

24. Samri, D. *Analyse Physique et Caracterisation Hygrothermique des Materiaux de Construction: Approche Experimentale et Modelisation Numerique* (in French). Ph.D. Dissertation, ENTPE: Lyon, France, 21 October 2008.
25. Pierre, T.; Colinart, T.; Glouannec, P. Measurements of thermal properties of biosourced building materials. In *Proceedings of the 18th Symposium on Thermophysical Properties*, Boulder, CO, USA, 24–29 June 2012.
26. Collet, F.; Pretot, S. Experimental investigation of moisture buffering capacity of sprayed hemp concrete. *Constr. Build. Mater.* **2012**, *36*, 58–65.
27. Shea, A.; Lawrence, M.; Walker, P. Hygrothermal performance of an experimental hemp-lime building. *Constr. Build. Mater.* **2012**, *36*, 270–275.
28. Tran Le, A.D.; Maalouf, C.; Mai, T.H.; Wurtz, E.; Collet, F. Transient hygrothermal behavior of a hemp concrete building envelope. *Energy Build.* **2010**, *30*, 1797–1806.
29. Maalouf, C.; Tran Le, A.D.; Lachi, M.; Wurtz, E.; Mai, T.H. Effect of moisture transfer on thermal inertia in simple layer walls: Case of a vegetal fibre material. *Math. Mod. Meth. Appl. Sci.* **2011**, *5*, 33–47.
30. Maalouf, C.; Tran Le, A.D.; Lachi, M.; Wurtz, E.; Mai, T.H. Effect of moisture transfer on heat energy storage in simple layer walls: Case of a vegetal fibre material. *Math. Mod. Meth. Appl. Sci.* **2011**, *5*, 1127–1134.
31. LIMATB Website. Available online: <http://web.univ-ubs.fr/limatb> (accessed on 17 January 2013).
32. Elfordy, S.; Lucas, F.; Tancret, F.; Scudeller, Y.; Goudet, L. Mechanical and thermal properties of lime and hemp concrete (“hemcrete”) manufactured by a projection process. *Constr. Build. Mater.* **2008**, *22*, 2116–2123.
33. Glouannec, P.; Chauvelon, P.; Colinart, T.; Le Bideau, P.; Zaknoune, A.; Jameline, N. Experimental and numerical studies of the drying of hemp concrete. In *Proceedings of the 17th International Drying Symposium*, Magdeburg, Germany, 3–6 October 2010;
34. Hedenblad, G. Measurement of moisture in high performance concrete. In *Proceedings of Nordic Concrete Federation Mini-Seminar “Moisture Measurement in Concrete Constructions Exposed to Temperature and Moisture Variations”*, Otaniemi, Espoo, Finland, 22 August 1997.
35. Peuhkuri, R.; Rode, C.; Hansen, K.K. Non-isothermal moisture transport through insulation materials. *Build. Environ.* **2008**, *43*, 811–822.
36. Hens, H. *Building Physics—Heat, Air and Moisture: Fundamentals and Engineering Methods with Examples and Exercises*; Ernst & Sohn: Berlin, Germany, 2007.